JACS
JOURNAL OF THE AMERICAN CHEMICAL SOCIETY
Article
Cite This: J. Am. Chem. Soc. 2019, 141, 1349−1358
pubs.acs.org/JACS

Spying on Neuronal Membrane Potential with Genetically Targetable Voltage Indicators

Vincent Grenier,[†] Brittany R. Daws,[‡] Pei Liu,[†] and Evan W. Miller*[,†,‡,§]

[†]Departments of Chemistry and [‡]Molecular & Cell Biology and [§]Helen Wills Neuroscience Institute, University of California, Berkeley, California 94720, United States

Supporting Information

ABSTRACT: Methods for optical measurement of voltage dynamics in living cells are attractive because they provide spatial resolution surpassing traditional electrode-based measurements and temporal resolution exceeding that of widely used Ca^{2+} imaging. Chemically synthesized voltage-sensitive dyes that use photoinduced electron transfer as a voltage-sensing trigger offer high voltage sensitivity and fast-response kinetics, but targeting chemical indicators to specific cells remains an outstanding challenge. Here, we present a new family of readily functionalizable, fluorescein-based voltage-sensitive fluorescent dyes (sarcosine-VoltageFluors) that can be covalently attached to a genetically encoded cell surface receptor to achieve voltage imaging from genetically defined neurons. We synthesized four new VoltageFluor derivatives that possess carboxylic acid functionality for simple conjugation to flexible tethers. The best of this new group of dyes was conjugated via a polyethylene glycol (PEG) linker to a small peptide (SpyTag, 13 amino acids) that directs binding and formation of a covalent bond with its binding partner, SpyCatcher (15 kDa). The new VoltageSpy dyes effectively label cells expressing cell-surface SpyCatcher, display good voltage sensitivity, and maintain fast-response kinetics. In cultured neurons, VoltageSpy dyes enable robust, single-trial optical detection of action potentials at neuronal soma with sensitivity exceeding genetically encoded voltage indicators. Importantly, genetic targeting of chemically synthesized dyes enables VoltageSpy to report on action potentials in axons and dendrites in single trials, tens to hundreds of micrometers away from the cell body. Genetic targeting of synthetic voltage indicators with VoltageSpy enables voltage imaging with low nanomolar dye concentration and offers a promising method for allying the speed and sensitivity of synthetic indicators with the enhanced cellular resolution of genetically encoded probes.

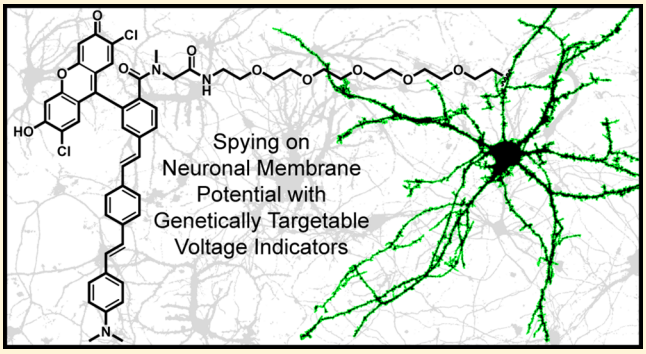

INTRODUCTION

Cellular membrane potential, or voltage, is a key physiological parameter critically important to all aspects of life, but especially to excitable cells, like neurons. Optical methods to image voltage promise to relieve our dependence on classic electrode-based methods, which are highly invasive, are often limited to single cells, and have extremely low throughput. Voltage-sensitive fluorescent indicators—either chemically synthesized or genetically encoded—offer an attractive solution for the direct observation of voltage dynamics in a minimally invasive, highly parallel, and high-throughput manner.[1,2]

Pioneering work showed that many commercially available dyes possess voltage-sensitive optical properties.[3−5] Targeted synthesis of voltage-sensitive compounds yielded dyes with voltage sensitivity arising from an electrochromic interaction between the fluorophore and the electric field across the membrane, or Stark effect.[6,7] These electrochromic dyes offer incredibly fast responses, but at the expense of relatively small shifts in their excitation/emission spectra. More recent versions display improved sensitivity but require torturous chemical syntheses.[8,9] Other chemical indicators include oxonol dyes which partition on the outer or inner leaflet of the plasma membrane in a voltage-dependent fashion. These dyes can give larger fractional changes in fluorescence, but oftentimes do not possess the required response kinetics to enable resolution of action potentials.[10−12] To address challenges associated with the speed and sensitivity of chemical dyes, we were inspired by elegant theoretical models[13] and early experimental examples,[14] to explore photoinduced electron transfer (PeT) through molecular wires as a modality for voltage sensing. These voltage-sensitive fluorophores, or VoltageFluors, developed in our lab are amenable to voltage sensing across a wide range of colors, afford high voltage sensitivities (up to 60% $\Delta F/F$ per 100 mV, in HEK cells), and maintain response times capable of clearly resolving action potential spikes in mammalian neurons.[15−19]

Completely genetically encoded approaches to voltage imaging offer a complementary method for voltage imag-

Received: November 8, 2018
Published: January 10, 2019

DOI: 10.1021/jacs.8b11997
J. Am. Chem. Soc. 2019, 141, 1349−1358

Scheme 1. Genetic Targeting of VoltageFluor Dyes Using SpyTag/SpyCatcher Methodology

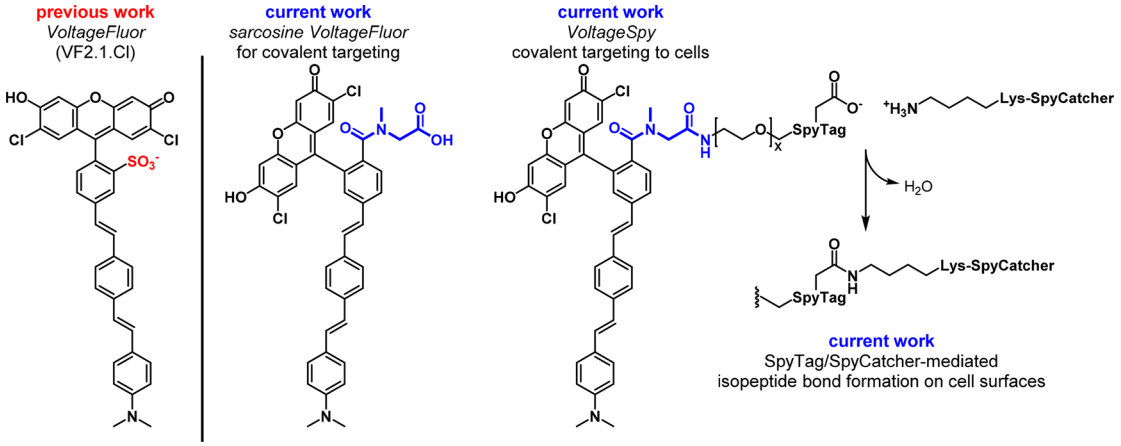

Scheme 2. Synthesis of Sarcosine VoltageFluors

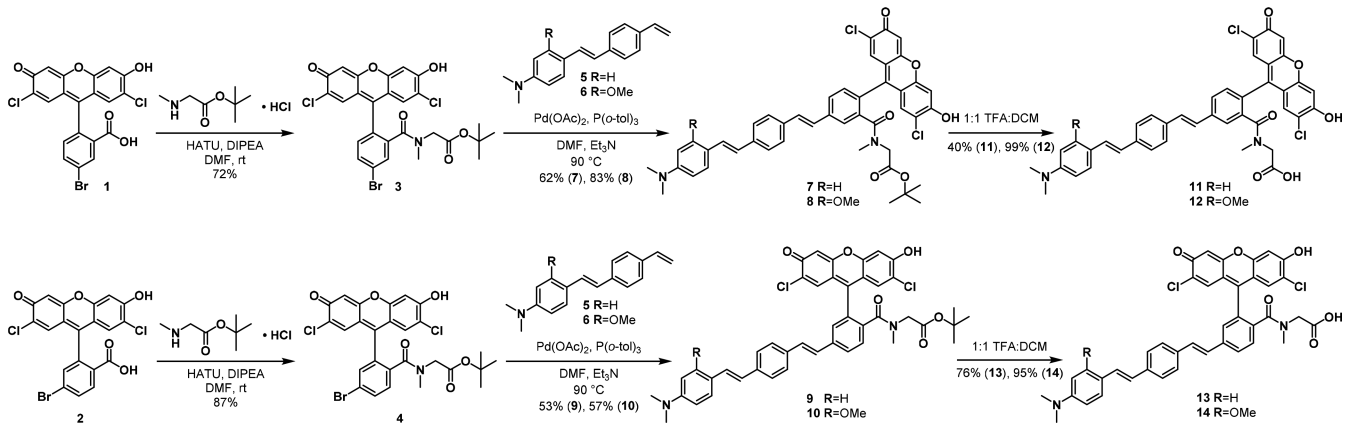

ing.[20,21] Genetically encoded platforms for voltage imaging cluster into three groups: fluorescent proteins coupled to voltage sensing domains from ion channels and/or enzymes,[22−27] opsin-based indicators,[28−32] or hybrid opsin-fluorescent protein fusions.[33−35] Improved trafficking[36] of fluorescent protein-based indicators enabled considerable improvement over early, pioneering protein-based voltage indicators.[22−24] Yet despite progress in recent years, significant challenges remain regarding proper trafficking of heterologous proteins to the cell membrane, response speed, low brightness, added capacitance, and/or light-induced ion pumping.

Hybrid chemical and genetic approaches to voltage imaging combine the speed and sensitivity of chemical indicators with the cell-type specificity of genetic model systems. Previous hybrid chemical-genetic methods for voltage sensing include the following: hybrid voltage sensor (hVOS) indicators in which an exogenously added, lipophilic anion partitions between inner and outer leaflets of the membrane in a voltage-dependent fashion to quench fluorescent protein fluorescence;[37−41] enzymatic localization in which genetically encoded phosphatases on the cell surface improve the membrane accumulation of a modified electrochromic dye;[42−44] electrochromic-FRET (eFRET) in which Cu-mediated click chemistry is employed to selectively attach a fluorophore to a picolyl azide incorporated on a voltage-sensitive opsin via an engineered lipoic acid ligase;[45] and a fluorogenic approach from our lab in which a genetically encoded esterase unmasks a caged VF dye in defined neurons (VoltageFluor activated by esterase Expression, VF-EX).[46] These approaches suffer variously from the following: the use of capacitance-adding anions like dipicrylamine; low selectivity in cell uptake and difficult chemical syntheses; toxicity associated with Cu-mediated catalysis on neuronal surfaces; and/or low contrast between cells which express the targeting enzyme and wild-type cells.

We hypothesized that we could address some of the shortcomings of our VF-EX targeting approach—specifically the low contrast between expressing and nonexpressing cells—by covalently tethering VF dyes to a cell of interest (Scheme 1). A number of excellent approaches exist for the covalent labeling of modified enzymes.[47−51] All rely on a modified enzyme that will label itself with a small, chemical ligand. We envisioned that one of these self-labeling enzymes could be targeted to the cell surface of a neuron of interest to direct covalent capture of a VF dye modified with the cognate ligand. We were specifically attracted to the SpyTag/SpyCatcher system[51] that employs an engineered cell adhesion molecule from *Streptococcus pyogenes*. The SpyTag fragment is a small peptide (13 amino acid residues) that interacts with the SpyCatcher enzyme to form an isopeptide bond. We hoped that by linking the SpyTag peptide to a VF dye via a flexible polyethylene glycol (PEG) linker, we could direct selective localization of VF dye only to those cells which express SpyCatcher on the cell surface. We additionally reasoned that use of the SpyTag peptide on VF would limit the amount of VF dye that passed through cell membranes, thus improving

DOI: 10.1021/jacs.8b11997
J. Am. Chem. Soc. 2019, 141, 1349−1358

Table 1. Properties of Sarcosine VF Dyes, PEGylated Intermediates, and VoltageSpy Indicators

dye	isomer	R	PEG units	λ_{max} (abs)[a]	λ_{max} (em)[a]	Φ[a]	cellular brightness[b]	contrast[b,c]	%ΔF/F[b,d]	effective sensitivity[e]
11	5	−H		525	541	2.7	10		27.2 ± 0.2	7
12	5	−OMe		525	540	5.5	1		12.2 ± 0.4	1
13	6	−H		525	540	3.9	40		22.7 ± 0.1	12
14	6	−OMe		524	540	0.8	6		29.3 ± 0.8	6
15	6	−H	3	526	545	5.8				
16	6	−H	11	526	544	10.9			3.2 ± 0.1	
17	6	−H	23	526	540	9.8				
18	6	−H	35	526	540	11.2				
19	6	−H	3	527	544	10.9		5.6 ± 3.8	12.5 ± 0.2[f]	
20	6	−H	11	526	544	7.9		12.6 ± 8.6	13.1 ± 0.2[f,g]	
21	6	−H	23	526	546	13.9		17.8 ± 9.7	11.6 ± 0.2[f]	
22	6	−H	35	526	546	8.7		34.6 ± 29.3	12.7 ± 0.1[f]	

[a]Acquired in PBS, pH 7.4 with 0.1% Triton X-100. [b]Measured in HEK cells. [c]Ratio of fluorescence intensity of SpyCatcher-expressing cells and median fluorescence intensity of untransfected cells loaded with 5 nM dye. Data is mean ± SD for 49−77 cells. [d]Per 100 mV step, optically sampled at 500 Hz. [e]Relative product of square root of cellular brightness and $\Delta F/F$. [f]Values are measured in HEK cells expressing cell-surface SpyCatcher. [g]In cells that do not express SpyCatcher, voltage sensitivity is 9.1 ± 0.1%.

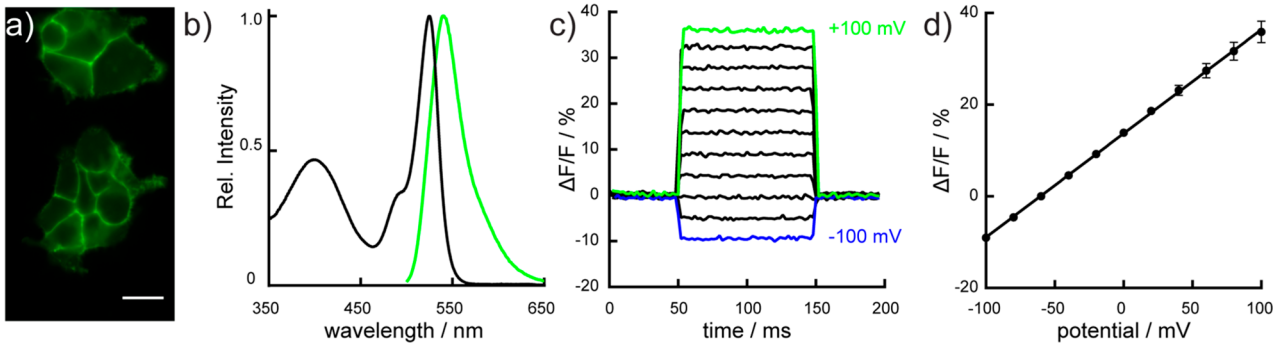

Figure 1. Characterization of sarcosine VoltageFluor dyes. (a) Widefield, fluorescence microscopy image of HEK cells loaded with 1 μM sarcosine probe **13**. Scale bar is 10 μM. (b) Absorbance (black line) and emission (green line) spectra of **13**. (c) Representative plot of fractional change in fluorescence ($\Delta F/F$) vs time from a series of voltage steps (+100 to −100 mV from a holding potential of −60 mV in 20 mV increments) recorded from a HEK cell stained with 1 μM **13** in whole-cell voltage clamp mode. (d) Plot of fractional change in fluorescence vs membrane potential from voltage-clamped HEK cells stained with 1 μM **13**. Data are mean ± SEM from six cells.

the membrane localization of the VF dye. Here, we show that SpyTag/SpyCatcher can be applied to a new VF scaffold to achieve fast and sensitive voltage imaging with only nanomolar concentrations of dye and in genetically defined neurons.

RESULTS

Synthesis of Sarcosine VoltageFluor Dyes. The structure of the prototypical green VoltageFluor VF2.1.Cl (Scheme 1) does not lend itself to further synthetic modification. We recently reported a family of rhodamine-based voltage reporters (RhoVRs) which have a sarcosine amide at the 3-position of the *meso* aromatic ring rather than an aryl sulfonate as in VF2.1.Cl.[18,52] The resultant free carboxylic acid offers a convenient handle for synthetic modification, maintains cellular impermeability, and is largely decoupled from the conjugated system of the phenylenevinylene molecular wire, making it a logical site for installing a targeting moiety (Scheme 1). The brightness and voltage sensitivity of VoltageFluor dyes are sensitive to the identity of the aniline electron donor[53] and orientation of the molecular wire.[17,54] To find an optimized green VoltageFluor which could serve as a starting point for our targeted voltage indicators, we synthesized and characterized a new series of sarcosine-containing VoltageFluor dyes (**11**−**14**) (Scheme 2). Starting from isomerically pure 5- and 6-bromo-2′,7′-dichlorofluorescein (**1**, **2**),[18,55] HATU-mediated amide couplings yielded *tert*-butyl ester protected intermediates **3** and **4** in 72% and 87% yield, respectively. Heck couplings with molecular wire fragments **5** or **6**[18] gave four *tert*-butyl ester protected VF-sarcosine compounds **7**−**10** in yields ranging from 53% to 83%. Removal of the *tert*-butyl ester with trifluoroacetic acid (TFA) gave sarcosinyl-VoltageFluors **11**−**14** in moderate to good yield (40%−99%) after purification by preparative thin layer chromatography (TLC). We confirmed sarcosinyl-VoltageFluors and their synthetic precursors form stable rotamer pairs using VT-NMR (spectra in the Supporting Information). All four sarcosine VF dyes (Table 1) displayed similar optical properties, with absorption and emission maxima centered at 525 and 540 nm, respectively. Quantum yields ranged from 0.008 (**12**) to 0.055 (**14**), in line with typical values for fluorescein-type VoltageFluors.[18,19]

Cellular Characterization of Sarcosine VoltageFluors. All the newly synthesized sarcosine VoltageFluors clearly labeled the plasma membranes of HEK cells (Figure 1, Figure S1) with variable fluorescence intensity. The brightest VF dye was **13**, displaying cellular fluorescence 40-fold greater than the dimmest indicator, **12** (Table 1, Figure S1). The voltage sensitivity of VoltageFluor-sarcosine probes was determined by dual optical and electrophysiology in HEK cells (Figure 1). We delivered voltage steps from +100 to −100 mV in 20 mV

DOI: 10.1021/jacs.8b11997
J. Am. Chem. Soc. 2019, 141, 1349−1358

Scheme 3. Synthesis of VoltageSpy Indicators

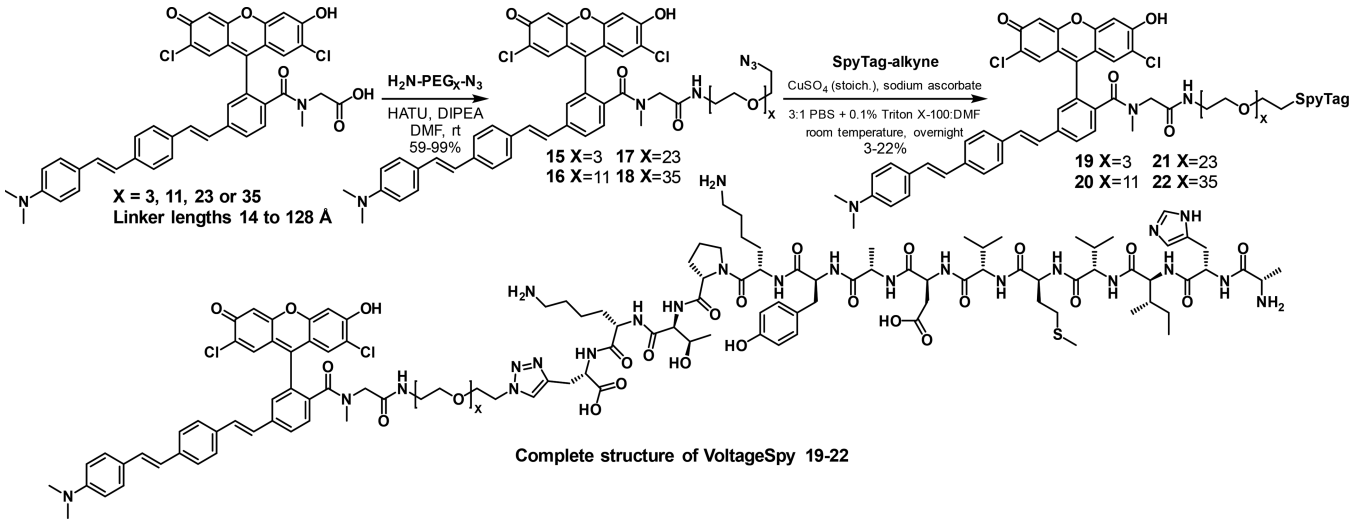

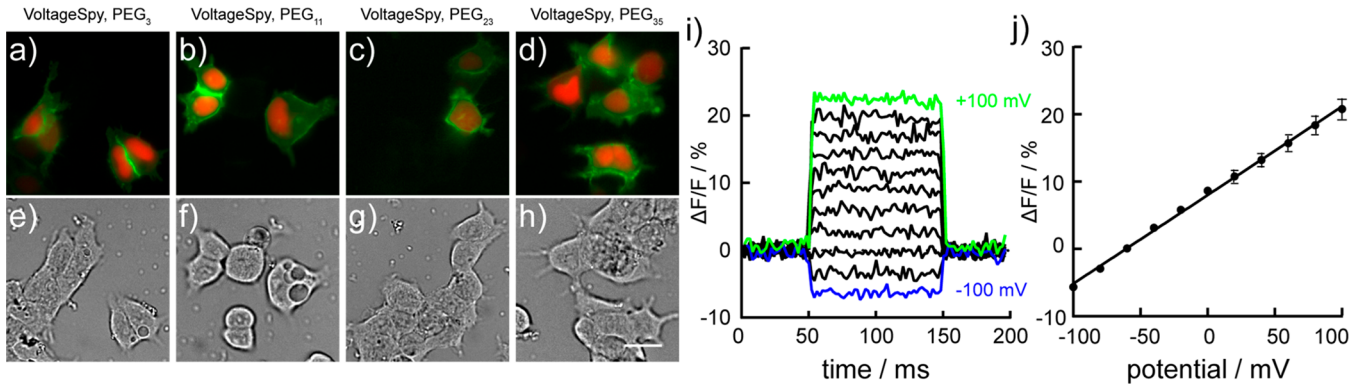

Figure 2. Evaluation of VoltageSpy dyes in HEK cells. (a–h) Wide-field fluorescence (a–d) and differential interference contrast (DIC) (e–h) microscopy images of HEK cells coexpressing SpyCatcher and nuclear mCherry (red signal) labeled with 5 nM VoltageSpy (green signal) dyes **19** (PEG_3; a, e), **20** (PEG_{11}; b, f), **21** (PEG_{23}; c, g), and **22** (PEG_{35}; d, h). Scale bar is 20 μm. (i) Representative plot of fractional change in fluorescence ($\Delta F/F$) vs time from a series of voltage steps (+100 to −100 mV from a holding potential of −60 mV in 20 mV increments) recorded from a HEK cell labeled with **22** in whole-cell voltage clamp mode. (j) Plot of fractional change in fluorescence vs membrane potential from voltage-clamped HEK cells labeled with **22**. Data are mean ± SEM from five cells.

increments to HEK293T in whole-cell voltage clamp while recording concomitant changes in fluorescence intensity over the cell body. Sarcosine VF **14** displayed the greatest voltage sensitivity, at 29% $\Delta F/F$ per 100 mV. The least sensitive was sarcosine VF **12**, at 12% $\Delta F/F$. Because sarcosine VF **13** possessed high cellular brightness, good voltage sensitivity, and superior signal-to-noise ratios (SNR) for detecting depolarizing voltage steps in HEK cells (Table 1, Figure 1, Figure S1), we thought it a promising candidate for covalent attachment to cell surfaces via SpyTag/SpyCatcher interaction.

Design and Synthesis of VoltageSpy Indicators. We envisioned that sarcosine VF **13** could be linked to the SpyTag peptide via a flexible PEG linker. The linker should be long enough to allow incorporation of the VF dye into the cell membrane. Because proper orientation of VF-type dyes in the cell membrane is critical for optimal voltage sensitivity,[17] the linker should ideally allow the dye to freely orient in the membrane. To assess this, we coupled sarcosine VF **13** to PEG linkers of lengths ranging from 14 to 128 Å (PEG_X; X = 3, 11, 23, or 35, Scheme 3). Amide coupling of sarcosine VF **13** with heterobifunctional PEG linkers terminating with amino and azido groups provided VF-PEG_X-N_3 intermediates **15**–**18** in 59–99% yields. PEGylation of **13** resulted in a small, linker-length-dependent red shift in the emission spectra, as well as an increase in quantum yield (Table 1, Figure S2). Copper-catalyzed azide–alkyne cyclization of compounds **15**–**18** with SpyTag-alkyne, in which the native SpyTag 13-mer peptide (AHIVMVDAYKPTK) is modified to contain propargyl glycine (Pra) on the C-terminus, resulting in the 14-residue peptide, AHIVMVDAYKPTK-Pra (SpyTag-Pra), gave VF-PEG_X-SpyTags **19**–**22** in 3–22% yield after purification by reversed-phase, semipreparative high-performance liquid chromatography (Scheme 3).

Evaluation of VoltageSpy Dyes in HEK Cells. To evaluate the performance of the new VF-PEG_X-SpyTags (VoltageSpy dyes), we expressed SpyCatcher on the surface of HEK cells. The SpyCatcher protein, originally engineered from the second immunoglobulin-like collagen adhesion domain (CnaB2) from the fibronectin binding protein FbaB of *Streptococcus pyogenes*, forms a stable isopeptide bond with SpyTag.[51] We hypothesized that the new VF-PEG_X-SpyTag dyes would be dependent on the presence of cell-surface SpyCatcher for effective membrane staining. We fused the original SpyCatcher protein to an N-terminal PAT3-derived

DOI: 10.1021/jacs.8b11997
J. Am. Chem. Soc. 2019, 141, 1349–1358

signal peptide[56] for efficient export from the cell and appended a C-terminal glycophosphatidyl inositol (GPI) anchor sequence derived from decay accelerating factor (DAF) (Figure S3).

SpyCatcher expression in HEK cells was confirmed by immunofluorescence directed against the hemagglutinin tag (HA) that was included at the N-terminus of the SpyCatcher protein (Figure S4a–d). To readily identify living cells expressing SpyCatcher, we included a nuclear-localized mCherry on the same gene, linked through the self-cleaving T2A linker to provide stoichiometric expression of nuclear mCherry alongside cell-surface SpyCatcher (Figure 2, Figure S3). VF-PEG$_X$-SpyTag conjugates **19**–**22** all show membrane labeling, with high selectivity for SpyCatcher expressing HEK293T cells over neighboring, nonexpressing cells (Figure 2, Figure S5). SpyCatcher permits the use of other signal peptides and transmembrane domains; plasmids employing a signal peptide from immunoglobulin κ (IgK) and platelet-derived growth factor receptor (PDGFR) also showed good surface expression of SpyCatcher in HEK293T cells (Figure S4e–k). The inclusion of the SpyTag peptide is essential for membrane localization: azido-PEG precursors **15**–**18** all show some degree of cellular internalization (Figure S6). This internalization lowers the nominal voltage sensitivity of the dyes; VF-PEG$_{11}$-N$_3$ shows only a modest 3% $\Delta F/F$ per 100 mV in HEK cells (Figure S6e).

SpyCatcher-Mediated Labeling of HEK Cells. VoltageSpy labeling of live HEK293T cells provides good contrast between SpyCatcher-expressing and nonexpressing cells (Figure 2a–h, Figure S5). At concentrations as low as 5 nM (2 orders of magnitude lower than typical loading concentrations for untargeted voltage-sensitive dyes), dyes of all PEG lengths gave mean contrast ratios ranging from 5.6 (±3.8, S.D., n = 77, PEG$_3$, VoltageSpy **19**) to 35 (±29, S.D., n = 50, PEG$_{35}$, VoltageSpy **22**). At a higher concentration of VoltageSpy, 25 nM, contrast ratios decreased, ranging from 3.9 (±1.9, S.D., n = 40, PEG$_3$, VoltageSpy **19**) to 13 (±8.8, S.D., n = 87, PEG$_{35}$, VoltageSpy **22**). At 100 nM VoltageSpy, contrast ratios decreased further to 3 (±1.9, S.D., n = 41, PEG$_{11}$, VoltageSpy **20**) and 7 (±4.1, S.D., n = 38, PEG$_{35}$, VoltageSpy **22**). The decrease in contrast ratio is driven by increasing amounts of nonspecific VoltageSpy labeling at higher dye concentrations. This nonspecific labeling is worse for short PEG linkers (X = 3, 11, VoltageSpy **19** and **20**) and is near negligible for the longer PEG linkers (X = 23, 35; VoltageSpy **21** and **22**) (Figure S5b). The fluorescence intensities of SpyCatcher-expressing cells do not substantially increase with addition of more VoltageSpy dye, indicating near saturation of available SpyCatcher binding sites, even at 5 nM VoltageSpy treatment (Figure S5a). The brighter regions that sometimes appear where two cell membranes touch (Figure 2a,b) are a result of imaging from a larger volume of vertical membrane at an interface using wide-field fluorescence microscopy. This is not an artifact of protein expression or labeling; we see a similar effect with the parent VoltageFluor (**13**, Figure 1a).

VoltageSpy Dependence on SpyCatcher. VoltageSpy labeling depends on the expression of cell surface SpyCatcher. Cellular VoltageSpy labeling could be blocked by preincubation of SpyCatcher-expressing cells with unlabeled SpyTag-peptide[51] (Figure S7). When VoltageSpy **20** (PEG$_{11}$) was applied to SpyCatcher-expressing cells pretreated with 10 μM SpyTag-Pra,[51] we observed a 62% decrease in membrane-associated fluorescence (Figure S7). The large excess of unlabeled SpyTag-Pra[51] required to block nanomolar concentrations of VoltageSpy suggests that the presence of a lipophilic molecular wire increases the labeling speed of VoltageSpy dyes. Partition of the molecular wire into the membrane may lead to a high local concentration of VoltageSpy at the cell surface, accelerating the SpyTag-SpyCatcher reaction and contributing to some of the background staining observed at higher VoltageSpy concentrations (Figure S5). We find that SpyTag conjugated to a simple dichlorofluorescein (Figure S8, DCF-PEG$_{11}$-SpyTag, **24**) applied at 100 nM gave only poor labeling of HEK cells, where micromolar concentrations of **24** were required to achieve appreciable labeling of SpyCatcher-expressing cells (Figure S8). However, in the absence of the lipophilic molecular wire, almost no off-target labeling was observed.

VoltageSpy Labels Extracellular Membrane Surfaces. The majority of the cellular fluorescence is associated with the extracellular face of the membrane. Treatment of VoltageSpy-labeled HEK cells (**22**, PEG$_{35}$, 5 nM) with Trypan Blue (0.1%) to quench extracellularly associated fluorescence[57] results in a 79% decrease in fluorescence intensity (Figure S9). In contrast, Trypan Blue treatment does not substantially decrease the fluorescence of a cytosolic fluorescent indicator, Oregon Green BAPTA (Figure S9), establishing that the majority of VoltageSpy fluorescence is associated with the external face of the plasma membrane. In this regard, VoltageSpy circumvents a common problem observed with genetically encoded voltage indicators; the presence of a substantial intracellular pool of improperly trafficked fluorophores which contribute a nonresponsive background signal.[36] Poor trafficking stymied the wide adoption of first-generation genetically encoded voltage indicators (GEVIs),[22−24,36] and improvements to the trafficking and subcellular targeting of GEVIs continue to advance the usefulness of fluorescent GEVIs.[32]

VoltageSpy dyes are voltage-sensitive after labeling SpyCatcher-expressing cells (Figure 2). VoltageSpy dyes **19**–**22** are all equally voltage-sensitive (25 nM dye), with a response of 12% $\Delta F/F$ per 100 mV (Table 2, Figure S10). We hypothesize that the small size of the SpyCatcher protein and the conformational flexibility of the C-terminus of SpyCatcher[58] enables even a PEG$_3$ linker (approximately 14 Å) to allow a VF dye to insert into the plasma membrane. Additionally, the final three amino acid residues of SpyTag project away from and do not form hydrogen bonds with SpyCatcher in the crystal structure,[58] providing additional flexibility for a tethered VF to reach the membrane. In HEK cells that do not express SpyCatcher, higher concentrations (1 μM) of VoltageSpy **20** are needed to stain the membrane. VoltageSpy **20** is voltage-sensitive in nonexpressing cells, at approximately 9% per 100 mV (Table 1, Figure S10e). Because the voltage sensitivity of the VoltageSpy dyes (9–13%) are lower than sarconsine VF **13** (22%), we hypothesize that the replacement of the anionic carboxylate on **13** with the neutral amide in **15**–**18** results in a slightly different orientation in the membrane,[17] decreasing voltage sensitivity. Conjugation to SpyCatcher may place additional constraints on the orientation of the VoltageFluor sensor.

VoltageSpy in Neurons. In neurons, VoltageSpy dyes recapitulate the selective staining observed in HEK293T cells. Using immunocytochemistry, we verified that the PAT3 signal sequence and the GPI sequence from DAF under control of the human synapsin promoter gave good cell-surface expression of SpyCatcher in cultured rat hippocampal neurons

DOI: 10.1021/jacs.8b11997
J. Am. Chem. Soc. 2019, 141, 1349−1358

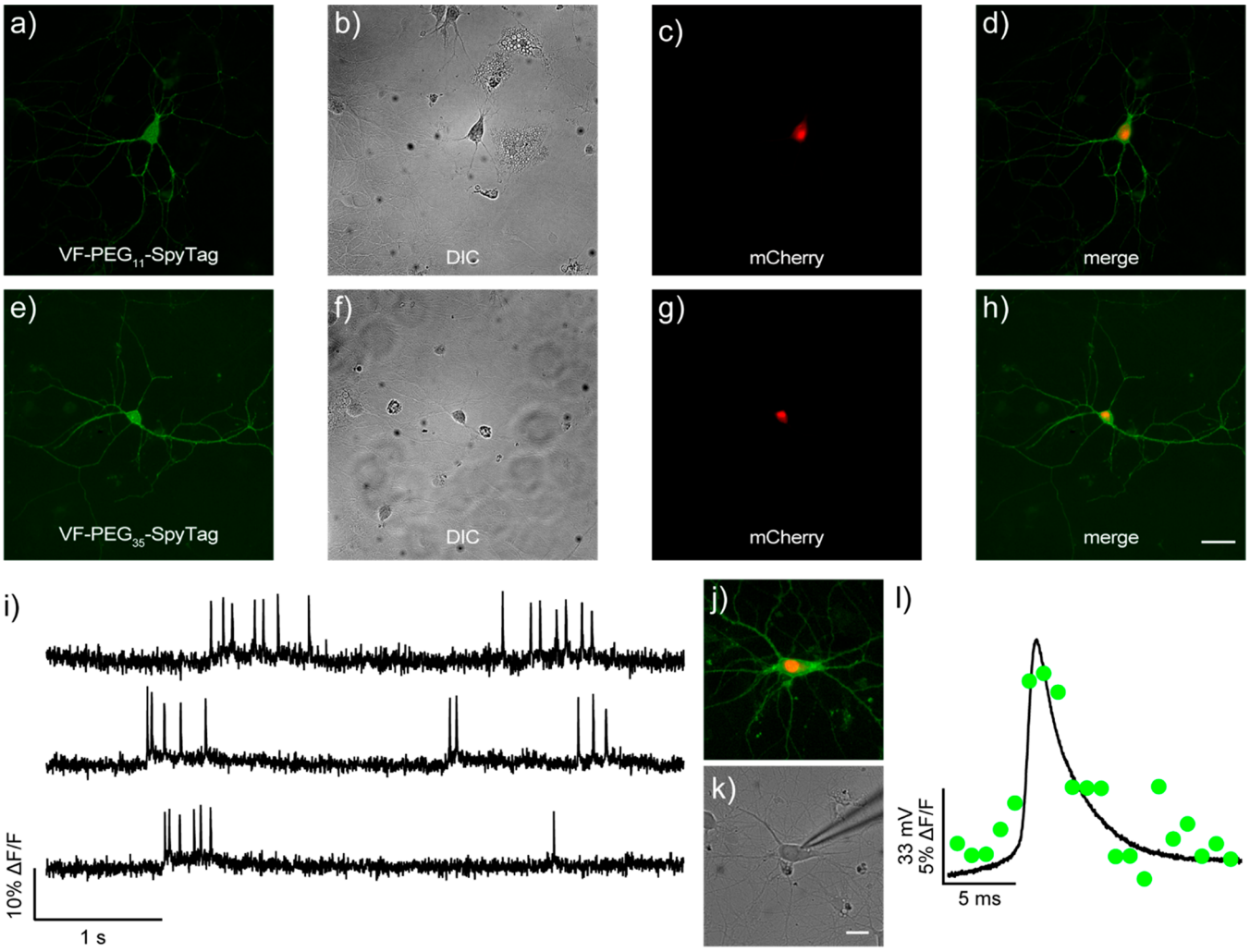

Figure 3. VoltageSpy dyes report on voltage dynamics in cultured hippocampal mammalian neurons. (a–h) Wide-field fluorescence and DIC microscopy images of neurons coexpressing SpyCatcher and nuclear mCherry labeled with VoltageSpy dyes **20** (a–d) and **22** (e–h). Scale bar is 40 μm. (i) Representative $\Delta F/F$ traces of spontaneous activity recorded from SpyCatcher expressing neurons labeled with **22**. Traces are $\Delta F/F$ from regions of interest at the cell bodies of neurons after background offset and bleach correction. Images were acquired at 500 Hz and represent single-trial acquisitions. Fluorescence ((j) merged VoltageSpy and mCherry signals) and DIC (k) microscopy images of a VoltageSpy **22** labeled neuron in whole-cell current-clamp mode. Scale bar is 20 μm. (l) Overlaid optical and electrophysiology signals from a single-action potential in a current-clamped neuron. Optical trace was acquired at 1 kHz.

(Figure S11). A combination of live-cell imaging followed by fixation and immunocytochemistry confirm the high specificity of the VoltageSpy/SpyCatcher interaction in neurons (Figure S11). Following live-cell staining with VoltageSpy **20** (PEG_{11}), membrane-associated VoltageSpy fluorescence survived fixation (Figure S11e,f), allowing us to establish good correlation between VoltageSpy localization and HA-epitope staining of SpyCatcher (Figure S11g–j). Live-cell imaging in neurons stained with VoltageSpy dyes (PEG_{11}, VoltageSpy **20**, Figure 3a–d; and PEG_{35}, VoltageSpy **22**, Figure 3e–h) showed good selectivity for SpyCatcher-expressing neurons over nonexpressing cells, with contrast ratios of approximately 5, across PEG lengths and concentrations (Figure S12). The contrast in neurons varied widely because of differences in SpyCatcher expression. The brightest neurons stained with VoltageSpy indicators possessed contrast ratios of approximately 25-fold over nontransfected cells; a 5-fold increase over contrast we achieved using fluorogenic VF dyes (ca. 4-fold in neurons).[46] We selected the brightest cells for subsequent imaging analysis.

Functional Imaging with VoltageSpy in Neurons. VoltageSpy dyes clearly report on action potentials from neurons expressing SpyCatcher. Under low-light illumination conditions (8 mW/mm^2) we successfully recorded spontaneous activity in cultured neurons with good signal to noise (Figure 3i). Both VoltageSpy **20** (PEG_{11}) and VoltageSpy **22** (PEG_{35}) readily recorded action potential spikes, with sensitivities of 11.6 ± 1.3% and 11.1 ± 1.4% $\Delta F/F$, respectively (Figure 3i, values are for n = 15 neurons and represent mean ± standard deviation, recorded at 500 Hz). The selectivity of targeting, lack of linker-length dependence on voltage sensitivity, and $\Delta F/F$ values in neurons match well with VoltageSpy performance in HEK cells. Dual optical and electrophysiological recordings of VoltageSpy **22** (PEG_{35}) reveal that targeted indicators faithfully report underlying action potential dynamics with no lag time (Figure 3j–l). Additionally, we established that the presence of either SpyCatcher alone or SpyCatcher + VoltageSpy did not alter neuronal membrane properties; we saw no difference in

DOI: 10.1021/jacs.8b11997
J. Am. Chem. Soc. 2019, 141, 1349–1358

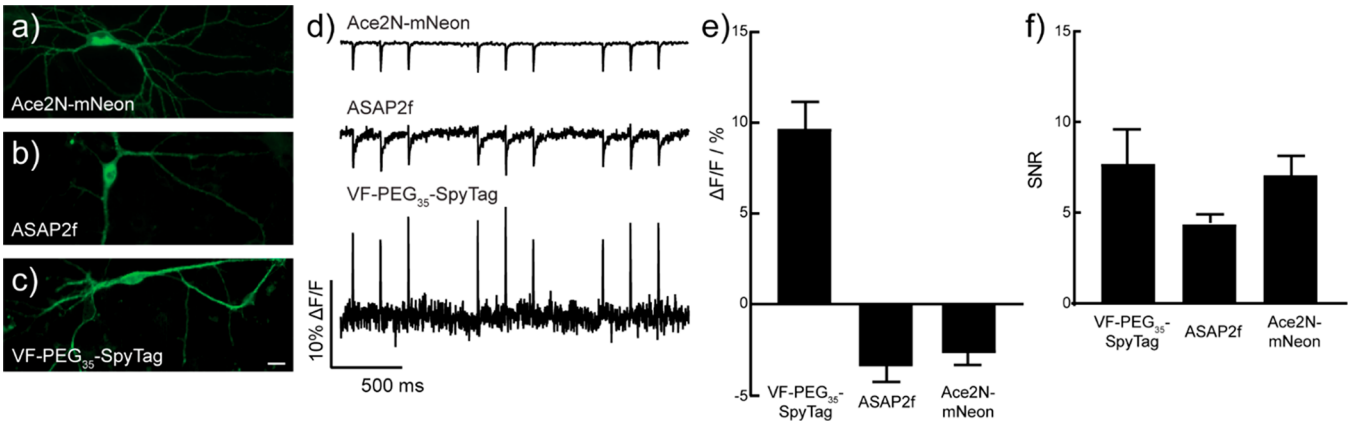

Figure 4. Comparison of VoltageSpy to GEVIs. Wide-field fluorescence microscopy images of cultured hippocampal neurons expressing (a) Ace2N-mNeon, (b) ASAP2f, or (c) SpyCatcher and labeled with VoltageSpy **22**. Scale bar is 20 μm. (d) Representative traces of optically recorded, evoked action potentials from each indicator recorded under identical imaging conditions. (e, f) Quantification of $\Delta F/F$ (e) and SNR (f) of evoked spikes. Data are mean ± SD for 17 (VoltageSpy), 15 (ASAP2f), and 15 (Ace2N-mNeon) cells and represent averaged $\Delta F/F$ and SNR values from all spikes in a single trace.

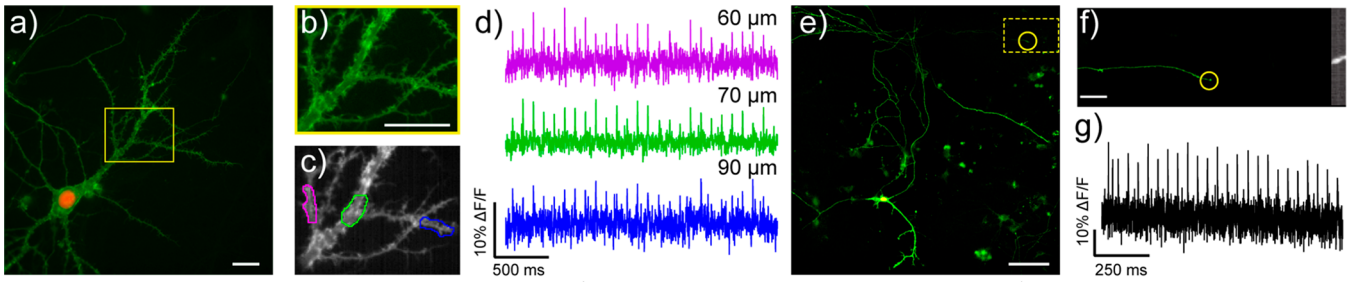

Figure 5. Subcellular voltage imaging with VoltageSpy dyes. (a–d) Imaging evoked action potentials in dendrites. (a) Wide-field fluorescence microscopy image of a hippocampal neuron coexpressing SpyCatcher and nuclear mCherry (red) and labeled with VoltageSpy **20** (green) under 63× magnification. Scale bar is 20 μm. (b) Close-up of boxed region in panel (a). Scale bar is 20 μm. (c) Average intensity projection of 2500 frames recorded at 500 Hz. Regions of interest (ROIs) are 10 μm long. d) ΔF/F traces of an evoked train of 25 APs. Color-coding corresponds to ROIs indicated in panel (c). Approximate distances from the center of the mCherry nucleus are indicated above each trace. (e–g) imaging evoked action potentials in axons. (e) Wide-field fluorescence microscopy image of a hippocampal neuron coexpressing SpyCatcher and nuclear mCherry (red channel) and labeled with VoltageSpy **20** (green signal) under 20× magnification. Scale bar is 100 μm. (f) Axon branch of the neuron in panel (e) under 63× magnification and close-up of axon terminal indicated by the yellow circle in panels (e) and (f) averaged intensity projection from 6000 frames imaged at 1.2 kHz. Scale bar is 10 μm. (g) $\Delta F/F$ trace of an evoked train of 25 APs recorded at 1.2 kHz.

membrane capacitance, resting membrane potential, or action potential kinetics (Figure S14).

VoltageSpy **22** (PEG_{35}) performs well in neurons, compared to other genetically encoded voltage indicators. VoltageSpy dyes possessed excellent sensitivity, detecting evoked action potential with 9.7 ± 1.5% $\Delta F/F$, compared to −2.7 ± 0.6% for ASAP2f,[59] a fluorescent protein-based indicator, and −3.4 ± 0.9% for Ace2N-mNeon,[60] an electrochromic FRET-based indicator (Figure 4) when all three indicators were imaged under identical conditions. Both ASAP2f and Ace2N-mNeon displayed negative-going responses to membrane depolarization, as a result of their sensing mechanism.[60,61] The SNR of VoltageSpy **22** for action potentials is 7.7 ± 1.9, comparable to Ace2N-mNeon (7.1 ± 1.1) and substantially larger than ASAP2f (4.4 ± 0.5) (Figure 4f). ASAP2f and Ace2N-mNeon are 2.4- and 15-fold brighter than VoltageSpy, respectively (as measured at the soma of cells from which we recorded), but the majority of the fluorescence of the genetically encoded indicators comes from fluorescence associated with internal structures—not the plasma membrane (Figure 4a–c, Figure S13). This highlights again a unique advantage of a hybrid approach in which a voltage-sensitive fluorophore is appended to a nonfluorescent genetically encoded membrane target: in the hybrid case of VoltageSpy/SpyCatcher, poorly trafficked proteins are invisible and do not contribute to unproductive background fluorescence.

Imaging Subcellular Voltage Dynamics. Measurements of the electronic properties of pre- and postsynaptic sites in neurons have been a tremendous, long-standing experimental challenge in neuroscience. Patching presynaptic boutons is difficult, and dendritic spines are inaccessible to electrophysiology. These structures therefore provide a unique opportunity where optical tools are the only viable existing method for interrogating their biology. The electric properties of dendrites have previously been probed with VSDs, but requires laborious internal loading of dyes via patch pipet.[62−66] GEVIs have also been employed to interrogate pre- and postsynaptic biology, but the slow kinetics and low brightness of GEVIs make these experiments challenging.[67]

By employing the speed and sensitivity of VF dyes with genetic targeting of the SpyTag/SpyCatcher system, we can readily image subcellular voltage dynamics in cultured hippocampal neurons. Application of 5 nM VoltageSpy **22** (PEG_{35}) results in clear, membrane-associated fluorescent restricted to SpyCatcher-expressing neurons indicated by nuclear mCherry (Figure 5a). VoltageSpy labeling discrim-

DOI: 10.1021/jacs.8b11997
J. Am. Chem. Soc. 2019, 141, 1349−1358

inates subcellular dendritic morphology—peripheral regions of dendrites are brighter than the internal cytosolic component (Figure 5b)—and micrometer-sized structures, dendritic spines, are visible (Figure 5b). Single-trial (no stimulus-timed averaging used) optical recordings of a train of 25 evoked action potentials imaged at dendritic sites (purple, green, and blue ROIs, Figure 5c) reveal clear action potentials (Figure 5d). VoltageSpy dyes enable remote monitoring of voltage dynamics in subcellular regions 60−90 μm away from neuronal soma, the site of traditional electrophysiological recordings (Figure 5d). In this way, genetically targeted VoltageSpy circumvents space clamp errors[68] associated with measuring voltage changes in structure that are not close to the neuronal cell body. In a complementary fashion, VoltageSpy **20** (PEG_{11}) can also image voltage dynamics in presynaptic structures associated with axon terminals (Figure 5e−g). The cellular specificity of the VoltageSpy/SpyCatcher interaction enables tracing of extensive axonal tracks (Figure 5e). Zooming in on the boxed region reveals the fine structure of an axon, several hundred micrometers distant from the nearest cell body (Figure 5f). Single-trial, high-speed imaging of 25 evoked action potentials clearly resolves fast voltage dynamics in a micrometer-sized axonal terminal hundreds of micrometers away from the neuronal soma (Figure 5g).

CONCLUSION

In conclusion, we show that voltage-sensitive fluorescent dyes can be covalently appended to the cell surface of mammalian cells and neurons, affording the opportunity for voltage imaging in genetically defined cells or in subcellular regions of interest. The best of the newly synthesized, sarcosine-containing VoltageFluors is readily functionalized with a PEG linker terminating with the SpyTag ligand. Localization of this VoltageSpy is determined by the expression of the SpyCatcher protein on cell surfaces. In this way, the speed and sensitivity of fluorescein-based voltage-sensitive fluorophores can be coupled with a genetically encoded component. This hybrid approach readily detects voltage changes in cultured cells and mammalian neurons. VoltageSpy performs well in cultured neurons, displaying up to 25-fold increase in staining in SpyCatcher-expressing cells, and reporting on action potentials with higher sensitivity than commonly used genetically encoded voltage indicators. With use of VoltageSpy, voltage dynamics in subcellular structures are readily observable in single-trial experiments—an experiment which is otherwise difficult in culture because of the extensive overlap of axons and dendrites from different neurons in any given area. The sparse labeling achieved with VoltageSpy dyes also points the way toward future experiments in brain slice and in vivo, where the high density of cell bodies and their processes complicate imaging from single cells with untargeted dyes. Looking forward, we aim to expand the palette of available VoltageSpy dyes by engaging carboxylate-containing rhodamine-based voltage reporters (RhoVRs),[52] develop new chemistries to target far-red dyes,[15] apply next-generation SpyTag/SpyCatcher constructs,[69] and mix and match complementary covalent targeting strategies[47−51] with our existing palette of voltage-sensitive dyes for multiplexed imaging in complex neural tissue.

ASSOCIATED CONTENT

Supporting Information

The Supporting Information is available free of charge on the ACS Publications website at DOI: 10.1021/jacs.8b11997.

Experimental details, synthetic procedures, imaging conditions, and supporting figures (PDF)

AUTHOR INFORMATION

Corresponding Author

*evanwmiller@berkeley.edu

ORCID

Evan W. Miller: 0000-0002-6556-7679

Notes

The authors declare no competing financial interest.

ACKNOWLEDGMENTS

Research in the Miller lab is supported in part by grants from the National Institutes of Health (R35GM119855, R01NS098088), National Science Foundation (NSF 1707350), and the Klingenstein-Simons Foundation (40746). V.G. is supported in part by a graduate fellowship from the Natural Sciences and Engineering Research Council of Canada. P.L. is supported by an A*STAR graduate fellowship. B.R.D. was supported in part by a training grant from the NIH (T32GM007232).

REFERENCES

(1) Peterka, D. S.; Takahashi, H.; Yuste, R. Imaging Voltage in Neurons. *Neuron* **2011**, *69* (1), 9−21.

(2) Scanziani, M.; Hausser, M. Electrophysiology in the age of light. *Nature* **2009**, *461* (7266), 930−939.

(3) Davila, H. V.; Salzberg, B. M.; Cohen, L. B.; Waggoner, A. S. Large Change in Axon Fluorescence That Provides a Promising Method for Measuring Membrane-Potential. *Nature-New Biol.* **1973**, *241* (109), 159−160.

(4) Salzberg, B. M.; Davila, H. V.; Cohen, L. B. Optical Recording of Impulses in Individual Neurons of an Invertebrate Central Nervous-System. *Nature* **1973**, *246* (5434), 508−509.

(5) Gupta, R. K.; Salzberg, B. M.; Grinvald, A.; Cohen, L. B.; Kamino, K.; Lesher, S.; Boyle, M. B.; Waggoner, A. S.; Wang, C. H. Improvements in Optical Methods for Measuring Rapid Changes in Membrane-Potential. *J. Membr. Biol.* **1981**, *58* (2), 123−137.

(6) Fluhler, E.; Burnham, V. G.; Loew, L. M. Spectra, Membrane-Binding, and Potentiometric Responses of New Charge Shift Probes. *Biochemistry* **1985**, *24* (21), 5749−5755.

(7) Loew, L. M.; Bonneville, G. W.; Surow, J. Charge Shift Optical Probes of Membrane-Potential - Theory. *Biochemistry* **1978**, *17* (19), 4065−4071.

(8) Hubener, G.; Lambacher, A.; Fromherz, P. Anellated hemicyanine dyes with large symmetrical solvatochromism of absorption and fluorescence. *J. Phys. Chem. B* **2003**, *107* (31), 7896−7902.

(9) Kuhn, B.; Fromherz, P. Anellated hemicyanine dyes in a neuron membrane: Molecular Stark effect and optical voltage recording. *J. Phys. Chem. B* **2003**, *107* (31), 7903−7913.

(10) Cacciatore, T. W.; Brodfuehrer, P. D.; Gonzalez, J. E.; Jiang, T.; Adams, S. R.; Tsien, R. Y.; Kristan, W. B., Jr.; Kleinfeld, D. Identification of neural circuits by imaging coherent electrical activity with FRET-based dyes. *Neuron* **1999**, *23* (3), 449−59.

(11) Gonzalez, J. E.; Tsien, R. Y. Voltage sensing by fluorescence resonance energy transfer in single cells. *Biophys. J.* **1995**, *69* (4), 1272−80.

(12) Gonzalez, J. E.; Tsien, R. Y. Improved indicators of cell membrane potential that use fluorescence resonance energy transfer. *Chem. Biol.* **1997**, *4* (4), 269−77.

(13) Li, L. S. Fluorescence probes for membrane potentials based on mesoscopic electron transfer. *Nano Lett.* **2007**, *7*, 2981−2986.

(14) De Silva, A. P.; Gunaratne, H. Q. N.; Habibjiwan, J. L.; Mccoy, C. P.; Rice, T. E.; Soumillion, J. P. New Fluorescent Model Compounds for the Study of Photoinduced Electron-Transfer - the

DOI: 10.1021/jacs.8b11997
J. Am. Chem. Soc. 2019, 141, 1349−1358

Influence of a Molecular Electric-Field in the Excited-State. *Angew. Chem., Int. Ed. Engl.* **1995**, *34* (16), 1728−1731.
(15) Huang, Y.-L.; Walker, A. S.; Miller, E. W. A Photostable Silicon Rhodamine Platform for Optical Voltage Sensing. *J. Am. Chem. Soc.* **2015**, *137*, 10767−10776.
(16) Kulkarni, R. U.; Kramer, D. J.; Pourmandi, N.; Karbasi, K.; Bateup, H. S.; Miller, E. W. Voltage-sensitive rhodol with enhanced two-photon brightness. *Proc. Natl. Acad. Sci. U. S. A.* **2017**, *114* (11), 2813−2818.
(17) Kulkarni, R. U.; Yin, H.; Pourmandi, N.; James, F.; Adil, M. M.; Schaffer, D. V.; Wang, Y.; Miller, E. W. A Rationally Designed, General Strategy for Membrane Orientation of Photoinduced Electron Transfer-Based Voltage-Sensitive Dyes. *ACS Chem. Biol.* **2017**, *12* (2), 407−413.
(18) Miller, E. W.; Lin, J. Y.; Frady, E. P.; Steinbach, P. A.; Kristan, W. B.; Tsien, R. Y. Optically monitoring voltage in neurons by photo-induced electron transfer through molecular wires. *Proc. Natl. Acad. Sci. U. S. A.* **2012**, *109* (6), 2114−2119.
(19) Woodford, C. R.; Frady, E. P.; Smith, R. S.; Morey, B.; Canzi, G.; Palida, S. F.; Araneda, R. C.; Kristan, W. B., Jr.; Kubiak, C. P.; Miller, E. W.; Tsien, R. Y. Improved PeT molecules for optically sensing voltage in neurons. *J. Am. Chem. Soc.* **2015**, *137* (5), 1817−24.
(20) Yang, H. H.; St-Pierre, F. Genetically Encoded Voltage Indicators: Opportunities and Challenges. *J. Neurosci.* **2016**, *36* (39), 9977−89.
(21) Lin, M. Z.; Schnitzer, M. J. Genetically encoded indicators of neuronal activity. *Nat. Neurosci.* **2016**, *19* (9), 1142−1153.
(22) Siegel, M. S.; Isacoff, E. Y. A genetically encoded optical probe of membrane voltage. *Neuron* **1997**, *19* (4), 735−41.
(23) Sakai, R.; Repunte-Canonigo, V.; Raj, C. D.; Knopfel, T. Design and characterization of a DNA-encoded, voltage-sensitive fluorescent protein. *Eur. J. Neurosci* **2001**, *13* (12), 2314−2318.
(24) Ataka, K.; Pieribone, V. A. A genetically targetable fluorescent probe of channel gating with rapid kinetics. *Biophys. J.* **2002**, *82* (1), 509−516.
(25) St-Pierre, F.; Marshall, J. D.; Yang, Y.; Gong, Y. Y.; Schnitzer, M. J.; Lin, M. Z. High-fidelity optical reporting of neuronal electrical activity with an ultrafast fluorescent voltage sensor. *Nat. Neurosci.* **2014**, *17* (6), 884−889.
(26) Jin, L.; Han, Z.; Platisa, J.; Wooltorton, J. R. A.; Cohen, L. B.; Pieribone, V. A. Single Action Potentials and Subthreshold Electrical Events Imaged in Neurons with a Fluorescent Protein Voltage Probe. *Neuron* **2012**, *75* (5), 779−785.
(27) Abdelfattah, A. S.; Farhi, S. L.; Zhao, Y. X.; Brinks, D.; Zou, P.; Ruangkittisakul, A.; Platisa, J.; Pieribone, V. A.; Ballanyi, K.; Cohen, A. E.; Campbell, R. E. A Bright and Fast Red Fluorescent Protein Voltage Indicator That Reports Neuronal Activity in Organotypic Brain Slices. *J. Neurosci.* **2016**, *36* (8), 2458−2472.
(28) Kralj, J. M.; Douglass, A. D.; Hochbaum, D. R.; Maclaurin, D.; Cohen, A. E. Optical recording of action potentials in mammalian neurons using a microbial rhodopsin. *Nat. Methods* **2012**, *9* (1), 90−U130.
(29) Hochbaum, D. R.; Zhao, Y.; Farhi, S. L.; Klapoetke, N.; Werley, C. A.; Kapoor, V.; Zou, P.; Kralj, J. M.; Maclaurin, D.; Smedemark-Margulies, N.; Saulnier, J. L.; Boulting, G. L.; Straub, C.; Cho, Y. K.; Melkonian, M.; Wong, G. K. S.; Harrison, D. J.; Murthy, V. N.; Sabatini, B. L.; Boyden, E. S.; Campbell, R. E.; Cohen, A. E. All-optical electrophysiology in mammalian neurons using engineered microbial rhodopsins. *Nat. Methods* **2014**, *11* (8), 825−833.
(30) Flytzanis, N. C.; Bedbrook, C. N.; Chiu, H.; Engqvist, M. K. M.; Xiao, C.; Chan, K. Y.; Sternberg, P. W.; Arnold, F. H.; Gradinaru, V. Archaerhodopsin variants with enhanced voltage-sensitive fluorescence in mammalian and Caenorhabditis elegans neurons. *Nat. Commun.* **2014**, *5*, 4894.
(31) Herwig, L.; Rice, A. J.; Bedbrook, C. N.; Zhang, R. J. K.; Lignell, A.; Cahn, J. K. B.; Renata, H.; Dodani, S. C.; Cho, I.; Cai, L.; Gradinaru, V.; Arnold, F. H. Directed Evolution of a Bright Near-Infrared Fluorescent Rhodopsin Using a Synthetic Chromophore. *Cell Chem. Biol.* **2017**, *24* (3), 415−425.
(32) Piatkevich, K. D.; Jung, E. E.; Straub, C.; Linghu, C. Y.; Park, D.; Suk, H. J.; Hochbaum, D. R.; Goodwin, D.; Pnevmatikakis, E.; Pak, N.; Kawashima, T.; Yang, C. T.; Rhoades, J. L.; Shemesh, O.; Asano, S.; Yoon, Y. G.; Freifeld, L.; Saulnier, J. L.; Riegler, C.; Engert, F.; Hughes, T.; Drobizhev, M.; Szabo, B.; Ahrens, M. B.; Flavell, S. W.; Sabatini, B. L.; Boyden, E. S. A robotic multidimensional directed evolution approach applied to fluorescent voltage reporters. *Nat. Chem. Biol.* **2018**, *14* (4), 352.
(33) Zou, P.; Zhao, Y. X.; Douglass, A. D.; Hochbaum, D. R.; Brinks, D.; Werley, C. A.; Harrison, D. J.; Campbell, R. E.; Cohen, A. E. Bright and fast multicoloured voltage reporters via electrochromic FRET. *Nat. Commun.* **2014**, *5*, 4625.
(34) Gong, Y. Y.; Wagner, M. J.; Li, J. Z.; Schnitzer, M. J. Imaging neural spiking in brain tissue using FRET-opsin protein voltage sensors. *Nat. Commun.* **2014**, *5*, 3674.
(35) Gong, Y. Y.; Huang, C.; Li, J. Z.; Grewe, B. F.; Zhang, Y. P.; Eismann, S.; Schnitzer, M. J. High-speed recording of neural spikes in awake mice and flies with a fluorescent voltage sensor. *Science* **2015**, *350* (6266), 1361−1366.
(36) Baker, B. J.; Lee, H.; Pieribone, V. A.; Cohen, L. B.; Isacoff, E. Y.; Knopfel, T.; Kosmidis, E. K. Three fluorescent protein voltage sensors exhibit low plasma membrane expression in mammalian cells. *J. Neurosci. Methods* **2007**, *161* (1), 32−38.
(37) Chanda, B.; Blunck, R.; Faria, L. C.; Schweizer, F. E.; Mody, I.; Bezanilla, F. A hybrid approach to measuring electrical activity in genetically specified neurons. *Nat. Neurosci.* **2005**, *8* (11), 1619−1626.
(38) Sjulson, L.; Miesenbock, G. Rational optimization and Imaging in vivo of a genetically encoded optical voltage reporter. *J. Neurosci.* **2008**, *28* (21), 5582−5593.
(39) Bayguinov, P. O.; Ma, Y. H.; Gao, Y.; Zhao, X. Y.; Jackson, M. B. Imaging Voltage in Genetically Defined Neuronal Subpopulations with a Cre Recombinase-Targeted Hybrid Voltage Sensor. *J. Neurosci.* **2017**, *37* (38), 9305−9319.
(40) Ghitani, N.; Bayguinov, P. O.; Ma, Y. H.; Jackson, M. B. Single-trial imaging of spikes and synaptic potentials in single neurons in brain slices with genetically encoded hybrid voltage sensor. *J. Neurophysiol.* **2015**, *113* (4), 1249−1259.
(41) Wang, D. S.; Zhang, Z.; Chanda, B.; Jackson, M. B. Improved Probes for Hybrid Voltage Sensor Imaging. *Biophys. J.* **2010**, *99* (7), 2355−2365.
(42) Hinner, M. J.; Hubener, G.; Fromherz, P. Enzyme-induced staining of biomembranes with voltage-sensitive fluorescent dyes. *J. Phys. Chem. B* **2004**, *108* (7), 2445−53.
(43) Hinner, M. J.; Hubener, G.; Fromherz, P. Genetic targeting of individual cells with a voltage-sensitive dye through enzymatic activation of membrane binding. *ChemBioChem* **2006**, *7* (3), 495−505.
(44) Ng, D. N.; Fromherz, P. Genetic targeting of a voltage-sensitive dye by enzymatic activation of phosphonooxymethyl-ammonium derivative. *ACS Chem. Biol.* **2011**, *6* (5), 444−51.
(45) Xu, Y. X.; Peng, L. X.; Wang, S. C.; Wang, A. Q.; Ma, R. R.; Zhou, Y.; Yang, J. H.; Sun, D. E.; Lin, W.; Chen, X.; Zou, P. Hybrid Indicators for Fast and Sensitive Voltage Imaging. *Angew. Chem., Int. Ed.* **2018**, *57* (15), 3949−3953.
(46) Liu, P.; Grenier, V.; Hong, W.; Muller, V. R.; Miller, E. W. Fluorogenic Targeting of Voltage-Sensitive Dyes to Neurons. *J. Am. Chem. Soc.* **2017**, *139* (48), 17334−17340.
(47) Los, G. V.; Encell, L. P.; McDougall, M. G.; Hartzell, D. D.; Karassina, N.; Zimprich, C.; Wood, M. G.; Learish, R.; Ohana, R. F.; Urh, M.; Simpson, D.; Mendez, J.; Zimmerman, K.; Otto, P.; Vidugiris, G.; Zhu, J.; Darzins, A.; Klaubert, D. H.; Bulleit, R. F.; Wood, K. V. HatoTag: A novel protein labeling technology for cell imaging and protein analysis. *ACS Chem. Biol.* **2008**, *3* (6), 373−382.
(48) Keppler, A.; Gendreizig, S.; Gronemeyer, T.; Pick, H.; Vogel, H.; Johnsson, K. A general method for the covalent labeling of fusion proteins with small molecules in vivo. *Nat. Biotechnol.* **2003**, *21* (1), 86−89.

DOI: 10.1021/jacs.8b11997
J. Am. Chem. Soc. 2019, 141, 1349−1358

(49) Gallagher, S. S.; Sable, J. E.; Sheetz, M. P.; Cornish, V. W. An In Vivo Covalent TMP-Tag Based on Proximity-Induced Reactivity. *ACS Chem. Biol.* **2009**, *4* (7), 547−556.
(50) Vivero-Pol, L.; George, N.; Krumm, H.; Johnsson, K.; Johnsson, N. Multicolor Imaging of cell surface proteins. *J. Am. Chem. Soc.* **2005**, *127* (37), 12770−12771.
(51) Zakeri, B.; Fierer, J. O.; Celik, E.; Chittock, E. C.; Schwarz-Linek, U.; Moy, V. T.; Howarth, M. Peptide tag forming a rapid covalent bond to a protein, through engineering a bacterial adhesin. *Proc. Natl. Acad. Sci. U. S. A.* **2012**, *109* (12), E690−7.
(52) Deal, P. E.; Kulkarni, R. U.; Al-Abdullatif, S. H.; Miller, E. W. Isomerically Pure Tetramethylrhodamine Voltage Reporters. *J. Am. Chem. Soc.* **2016**, *138* (29), 9085−8.
(53) Woodford, C. R.; Frady, E. P.; Smith, R. S.; Morey, B.; Canzi, G.; Palida, S. F.; Araneda, R. C.; Kristan, W. B.; Kubiak, C. P.; Miller, E. W.; Tsien, R. Y. Improved PeT molecules for optically sensing voltage in neurons. *J. Am. Chem. Soc.* **2015**, *137*, 1817−24.
(54) Deal, P. E.; Kulkarni, R. U.; Al-Abdullatif, S. H.; Miller, E. W. Isomerically Pure Tetramethylrhodamine Voltage Reporters. *J. Am. Chem. Soc.* **2016**, *138*, 9085−9088.
(55) Jiao, G. S.; Han, J. W.; Burgess, K. Syntheses of regioisomerically pure 5- or 6-halogenated fluoresceins. *J. Org. Chem.* **2003**, *68* (21), 8264−7.
(56) Kim, J.; Zhao, T.; Petralia, R. S.; Yu, Y.; Peng, H.; Myers, E.; Magee, J. C. mGRASP enables mapping mammalian synaptic connectivity with light microscopy. *Nat. Methods* **2012**, *9* (1), 96−102.
(57) Wakayama, S.; Kiyonaka, S.; Arai, I.; Kakegawa, W.; Matsuda, S.; Ibata, K.; Nemoto, Y. L.; Kusumi, A.; Yuzaki, M.; Hamachi, I. Chemical labelling for visualizing native AMPA receptors in live neurons. *Nat. Commun.* **2017**, *8*, 14850.
(58) Li, L.; Fierer, J. O.; Rapoport, T. A.; Howarth, M. Structural analysis and optimization of the covalent association between SpyCatcher and a peptide Tag. *J. Mol. Biol.* **2014**, *426* (2), 309−17.
(59) Yang, H. H.; St-Pierre, F.; Sun, X.; Ding, X.; Lin, M. Z.; Clandinin, T. R. Subcellular Imaging of Voltage and Calcium Signals Reveals Neural Processing In Vivo. *Cell* **2016**, *166* (1), 245−57.
(60) Gong, Y.; Huang, C.; Li, J. Z.; Grewe, B. F.; Zhang, Y.; Eismann, S.; Schnitzer, M. J. High-speed recording of neural spikes in awake mice and flies with a fluorescent voltage sensor. *Science* **2015**, *350* (6266), 1361−6.
(61) St-Pierre, F.; Marshall, J. D.; Yang, Y.; Gong, Y.; Schnitzer, M. J.; Lin, M. Z. High-fidelity optical reporting of neuronal electrical activity with an ultrafast fluorescent voltage sensor. *Nat. Neurosci.* **2014**, *17* (6), 884−9.
(62) Antic, S.; Zecevic, D. Optical Signals from Neurons with Internally Applied Voltage-Sensitive Dyes. *J. Neurosci.* **1995**, *15* (2), 1392−1405.
(63) Yan, P.; Acker, C. D.; Zhou, W. L.; Lee, P.; Bollensdorff, C.; Negrean, A.; Lotti, J.; Sacconi, L.; Antic, S. D.; Kohl, P.; Mansvelder, H. D.; Pavone, F. S.; Loew, L. M. Palette of fluorinated voltage-sensitive hemicyanine dyes. *Proc. Natl. Acad. Sci. U. S. A.* **2012**, *109* (50), 20443−20448.
(64) Roome, C. J.; Kuhn, B. Simultaneous dendritic voltage and calcium imaging and somatic recording from Purkinje neurons in awake mice. *Nat. Commun.* **2018**.
(65) Bradley, J.; Luo, R.; Otis, T. S.; DiGregorio, D. A. Submillisecond Optical Reporting of Membrane Potential In Situ Using a Neuronal Tracer Dye. *J. Neurosci.* **2009**, *29* (29), 9197−9209.
(66) Fink, A. E.; Bender, K. J.; Trussell, L. O.; Otis, T. S.; DiGregorio, D. A., Two-Photon Compatibility and Single-Voxel, Single-Trial Detection of Subthreshold Neuronal Activity by a Two-Component Optical Voltage Sensor. *PLoS One* **2012**, *7* (8).e41434
(67) Hoppa, M. B.; Gouzer, G.; Armbruster, M.; Ryan, T. A. Control and Plasticity of the Presynaptic Action Potential Waveform at Small CNS Nerve Terminals. *Neuron* **2014**, *84* (4), 778−789.
(68) Spruston, N.; Jaffe, D. B.; Williams, S. H.; Johnston, D. Voltage- and space-clamp errors associated with the measurement of electrotonically remote synaptic events. *J. Neurophysiol.* **1993**, *70* (2), 781−802.
(69) Keeble, A. H.; Banerjee, A.; Ferla, M. P.; Reddington, S. C.; Anuar, I.; Howarth, M. Evolving Accelerated Amidation by SpyTag/SpyCatcher to Analyze Membrane Dynamics. *Angew. Chem., Int. Ed.* **2017**, *56* (52), 16521−16525.

DOI: 10.1021/jacs.8b11997
J. Am. Chem. Soc. 2019, 141, 1349−1358